Preparation, X-ray Crystallography, and Thermal Decomposition of Some Transition Metal Perchlorate Complexes of Hexamethylenetetramine †

ARTICLE *in* THE JOURNAL OF PHYSICAL CHEMISTRY A · JANUARY 2008

Impact Factor: 2.69 · DOI: 10.1021/jp077278z · Source: PubMed

5 AUTHORS, INCLUDING:

Gurdip Singh
Deen Dayal Upadhyaya Gorakhpur University
325 PUBLICATIONS **3,564** CITATIONS
SEE PROFILE

Dinesh Kumar
Department Of Electronics And Information…
10 PUBLICATIONS **98** CITATIONS
SEE PROFILE

Preparation, X-ray Crystallography, and Thermal Decomposition of Some Transition Metal Perchlorate Complexes of Hexamethylenetetramine†

Gurdip Singh,* B. P. Baranwal, I. P. S. Kapoor, and Dinesh Kumar

Department of Chemistry, DDU Gorakhpur University, Gorakhpur 273009, India

Roland Fröhlich

Organisch-Chemisches Institut, Universität Münster, D-48149 Münster, Germany

Received: September 11, 2007; In Final Form: October 4, 2007

The perchlorate complexes of manganese, nickel, and zinc with hexamethylenetetramine (HMTA) of the general formula $[M(H_2O-HMTA-H_2O)_2(H_2O-ClO_4)_2(H_2O)_2]$ (where M = Mn, Ni, and Zn) have been prepared and characterized by X-ray crystallography. Thermal studies were undertaken using thermogravimetry (TG), differential thermal analysis (DTA), and explosion delay (D_E) measurements. The kinetics of thermal decomposition of these complexes was investigated using isothermal TG data by applying isoconversional method. The decomposition pathways of the complexes have also been proposed. These were found to explode when subjected to higher temperatures.

Introduction

Hexamethylenetetramine (HMTA) known as urotropine or tetraazaadamantane (taad) in which four nitrogen atoms are situated at the corners of a tetrahedron, is a ligand of polycyclicpolydentate type. In many complexes, it acts as a monodentate[1] or bidentate ligands[2,3] and shows nonchelating behavior[4] (in low valent organometallic complexes). It is used for preparing RDX. Studies on the thermolysis and kinetics of some of the transition metal nitrate and perchlorate complexes with 1,4-diaminobutane,[5,6] propylenediamine,[7,8] ethylenediamine[9,10] and 1,6-diaminohexane as ligand[11] have already been reported. We have previously investigated the thermal decomposition and ignition characteristics of metal nitrate complexes having intermolecular hydrogen-bonded HMTA.[12]

The metal amine complexes having ClO_4^- as counterion undergoes self-propagative decomposition reactions due to presence of both oxidizing (ClO_4^-) and reducing groups in the same molecules.[6,8,10] On the basis of their sensitivity, amine perchlorate complexes lie in between primary and secondary explosives.[13] These complexes at higher temperature decompose to form metal oxide with evolution of gaseous products. These ultrafine metal oxides have interesting electrical, magnetic and catalytic properties.[14] Hence, transition metal complexes have been found to be potential burning rate modifier for HTPB-AP propellants.[15,16] In this paper, we report the preparation, crystal structure, thermal decomposition, and explosion characteristic of the transition metal perchlorate complexes having hydrogen-bonded HMTA moiety.

Experimental Section

Materials. All commercially available chemicals are of AR grade, zinc carbonate (s.d. fine), manganese carbonate (Thomas baker), nickel carbonate, silica gel TLC grade (Qualigens), 70% perchloric acid (Merck), and HMTA (Lancaster) were used as received.

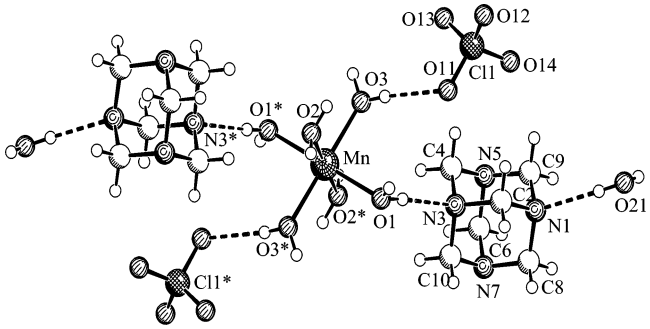

Figure 1. Crystal structure of the Mn complex.

Preparation of the Complexes. Hexahydrate metal perchlorate salts were crystallized by treating corresponding metal carbonates with 70% perchloric acid. After being washed with petroleum ether, these salts were recrystallized from distilled water and finally dried under vacuum over fused calcium chloride. The metal perchlorate complexes were prepared by treating the aqueous solution of metal perchlorate hexahydrate salts with HMTA in appropriate stoichiometric ratio. These complexes were recrystallized from water and dried. The molar conductances of the complexes have been measured on Century CC 601 in water as well as dimethylsulphoxide (DMSO).

X-ray Crystallographic Study. Crystals of the complexes were obtained by the recrystallization from aqueous solutions. The data collection of the crystals were performed at low temperature (198 K) using a Nonius Kappa CCD diffractometer, equipped with a rotating anode generator Nonius FR591. Programs used: involves data collection Collect (Nonius B.V.; 1998), data reduction and absorption correction Denzo-SMN.[17] The structures were solved by direct methods SHELXS-97[18] and refined by full-matrix least-squares method on all F^2 data using SHELXL-97.[19] Hydrogen atoms were placed on calculated

* Corresponding author. E-mail: gsingh4us@yahoo.com. Phone: 91-551-2200745 (R) 2202856 (O). Fax: 91-551-2340459.

† Part 57.

10.1021/jp077278z CCC: $37.00
Published on Web 11/22/2007

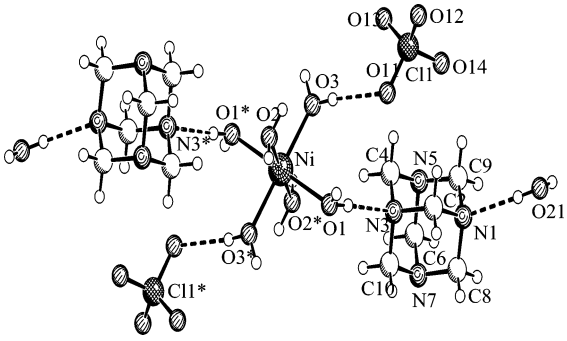

Figure 2. Crystal structure of the Ni complex.

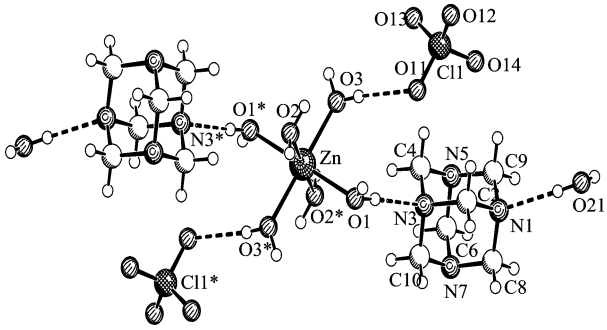

Figure 3. Crystal structure of the Zn complex.

positions and refined riding; at the water molecules they were located from a difference Fourier map and refined independently. Refinement with anisotropic thermal parameters for non-hydrogen atoms led to the *R* values of 0.049 (Mn), 0.051 (Ni), and 0.045 (Zn). The crystal structures (graphics done with Schakal[20]) of the complexes are shown in the Figures 1−3. The crystal data, structure refinement, bond lengths, and bond angles for complexes are summarized in Tables 1 and 2.

Thermal Analysis of the Complexes. TG was taken at 5 °C/min in a static air atmosphere (sample mass 20 mg, 100−200 mesh) on indigenously fabricated TG apparatus[21] (Figure 4). DTA was done in a static air atmosphere on a Universal Thermal Analysis instrumentt(sample mass ∼20 mg, heating rate 10 °C/min) (Figure 5). TG and DTA phenomenological data are summarized in Table 3. Isothermal TG was performed at appropriate temperatures in static air (mass ∼20 mg) using a gold crucible as the sample holder, and thermograms are shown in Figure 6. The explosion delay (D_E) data were recorded using tube furnace technique[22] (mass 20 mg, 100−200 mesh) in the temperature range 280−360 °C. The accuracy of the temperature of the tube furnace was ±1 °C. Each run was repeated five times, and mean D_E values are reported in Table 4. The D_E data were found to fit in the following equation:[23−25]

$$D_E = Ae^{E^*/RT}$$

where E^* is the activation energy for explosion and T is the absolute temperature. A plot of ln D_E vs $1/T$ is shown in Figure 7.

Kinetic Analysis of Isothermal TG Data. Isothermal TG data were used to evaluate kinetics of thermolysis by model fitting[26] as well as the model free isoconversional method given by Vyazovkin and Wight.[27] The following equation was found to fit the isothermal TG data

$$-\ln t_{\alpha,i} = \ln[A/g(\alpha)] - E/RT_i$$

TABLE 1: Crystal and Structure Refinement Data

complex designation	Mn complex	Ni complex	Zn complex
empirical formula	$C_{12}H_{40}Cl_2MnN_8O_{16}$	$C_{12}H_{40}Cl_2N_8NiO_{16}$	$C_{12}H_{40}Cl_2N_8O_{16}Zn$
color	colorless	light green	colorless
formula weight	678.36	682.13	688.79
temp/K	198(2)	198(2)	198(2)
λ/Å	0.71073	0.71073	0.71073
crystal system	triclinic	triclinic	triclinic
space group	$P\bar{1}$ (No. 2)	$P\bar{1}$ (No. 2)	$P\bar{1}$ (No. 2)
cell constants	a = 8.3050(2) Å	a = 8.1778(1) Å	a = 8.2148(1) Å
	α = 93.921(1)°	α = 93.955(1)°	α = 93.856(1)°
	b = 9.1845(2) Å	b = 9.1073(1) Å	b = 9.1318(2) Å
	β = 104.338(1)°	β = 104.417(1)°	β = 104.497(1)°
	c = 10.7325(2) Å	c = 10.6844(2) Å	c = 10.7006(2) Å
	γ = 113.913(1)°	γ = 113.892(2)°	γ = 113.859(1)°
volume	711.78(3) Å^3	691.57(2) Å^3	697.75(2) Å^3
molecules per unit cell, Z	1	1	1
calculated density	1.583 Mg/m^3	1.638 Mg/m^3	1.639 Mg/m^3
absorption coefficient	0.733 mm^{-1}	0.978 mm^{-1}	1.155 mm^{-1}
F(000)	355	358	360
crystal size/nm	0.35 × 0.20 × 0.15	0.40 × 0.30 × 0.15	0.65 × 0.60 × 0.10
θ range for data collection	2.47 to 28.28°	2.49 to 27.64°	2.00to 28.24°
limiting indices	$-11 \le h \le 11$	$-10 \le h \le 9$	$-7 \le h \le 10$
	$-12 \le k \le 11$	$-10 \le k \le 11$	$-11 \le k \le 10$
	$-14 \le l < 13$	$-13 \le l \le 14$	$-14 \le l \le 13$
reflections collected/unique	6631/3427	7503/3212	6824/3317
	[R(int) = 0.031]	[R(int) = 0.049]	[R(int) = 0.040]
reflections observed [$I > 2\sigma(I)$]	3003	3022	3158
data/restraints/parameters	3427/0/210	3212/0/210	3317/0/211
goodness-off-fit on F^2	1.073	1.056	1.075
final R indices [$I > 2\sigma(I)$]	$R1$ = 0.0489	$R1$ = 0.051	$R1$ = 0.045
	wR^2 = 0.120	wR^2 = 0.129	wR^2 = 0.118
R indices (all data)	$R1$ = 0.056	$R1$ = 0.054	$R1$ = 0.047
	wR^2 = 0.126	wR^2 = 0.131	wR^2 = 0.120
extinction coefficient	none	none	0.183(11)
largest diff. peak and hole/e Å^{-3}	+1.17 and −1.07	+1.21 and −1.20	+1.16 and −1.12
CCDC no.	658325	658324	658326

TABLE 2: Bond Lengths (Å) and Angles (deg) for Complexes[a]

Mn complex		Ni complex		Zn complex	
bond	bond length	bond	bond length	bond	bond length
Mn−O(3)#1	2.1540(18)	Ni−O(3)#1	2.0390(19)	Zn−O(3)#1	2.0704(18)
Mn−O(3)	2.1540(18)	Ni−O(3)	2.0390(19)	Zn−O(3)	2.0704(18)
Mn−O(1)#1	2.1666(18)	Ni−O(1)#1	2.0469(18)	Zn−O(1)#1	2.0729(17)
Mn−O(1)	2.1666(18)	Ni−O(1)	2.0469(18)	Zn−O(1)	2.0729(17)
Mn−O(2)	2.1947(17)	Ni−O(2)	2.0712(18)	Zn−O(2)#1	2.1174(17)
Mn−O(2)#1	2.1947(17)	Ni−O(2)#1	2.0712(18)	Zn−O(2)	2.1174(17)
Cl(1)−O(14)	1.388(3)	Cl(1)−O(14)	1.389(3)	Cl(1)−O(14)	1.389(3)
Cl(1)−O(12)	1.399(3)	Cl(1)−O(13)	1.392(4)	Cl(1)−O(12)	1.396(3)
Cl(1)−O(13)	1.399(3)	Cl(1)−O(12)	1.395(3)	Cl(1)−O(13)	1.397(3)
Cl(1)−O(11)	1.439(2)	Cl(1)−O(11)	1.439(2)	Cl(1)−O(11)	1.444(2)
N(1)−C(8)	1.472(3)	N(1)−C(8)	1.472(3)	N(1)−C(8)	1.474(3)
N(1)−C(2)	1.474(3)	N(1)−C(2)	1.475(3)	N(1)−C(2)	1.475(3)
N(1)−C(9)	1.474(3)	N(1)−C(9)	1.477(3)	N(1)−C(9)	1.478(3)
C(2)−N(3)	1.478(3)	C(2)−N(3)	1.478(3)	C(2)−N(3)	1.476(3)
N(3)−C(4)	1.474(3)	N(3)−C(10)	1.473(3)	N(3)−C(10)	1.473(3)
N(3)−C(10)	1.476(3)	N(3)−C(4)	1.473(3)	N(3)−C(4)	1.478(3)
C(4)−N(5)	1.476(3)	C(4)−N(5)	1.477(3)	C(4)−N(5)	1.478(3)
N(5)−C(6)	1.474(3)	N(5)−C(6)	1.473(3)	N(5)−C(6)	1.473(3)
N(5)−C(9)	1.479(3)	N(5)−C(9)	1.478(3)	N(5)−C(9)	1.477(3)
C(6)−N(7)	1.474(3)	C(6)−N(7)	1.474(3)	C(6)−N(7)	1.476(3)
N(7)−C(10)	1.474(3)	N(7)−C(10)	1.475(3)	N(7)−C(10)	1.476(3)
N(7)−C(8)	1.480(3)	N(7)−C(8)	1.480(3)	N(7)−C(8)	1.482(3)

Mn complex		Ni complex		Zn complex	
bond	bond angle	bond	bond angle	bond	bond angle
O(3)#1−Mn−O(3)	180.00(11)	O(3)#1−Ni−O(3)	180.00(18)	O(3)#1−Zn−O(3)	180.00(17)
O(3)−Mn−O(1)#1	91.49(7)	O(3)−Ni−O(1)#1	90.04(8)	O(3)−Zn−O(1)#1	90.23(8)
O(3)#1−Mn−O(1)	91.49(7)	O(3)#1−Ni−O(1)	90.04(8)	O(3)#1−Zn−O(1)	90.23(8)
O(3)−Mn−O(1)	88.51(7)	O(3)−Ni−O(1)	89.96(8)	O(3)−Zn−O(1)	89.77(8)
O(1)#1−Mn−O(1)	180.0	O(1)#1−Ni−O(1)	180.00(12)	O(1)#1−Zn−O(1)	180.00(11)
O(3)#1−Mn−O(2)	91.09(8)	O(3)#1−Ni−O(2)	89.75(9)	O(3)#1−Zn−O(2)#1	89.77(8)
O(3)−Mn−O(2)	88.91(8)	O(3)−Ni−O(2)	90.25(9)	O(3)−Zn−O(2)#1	90.23(8)
O(1)#1−Mn−O(2)	91.31(7)	O(1)#1−Ni−O(2)	89.60(8)	O(1)#1−Zn−O(2)#1	90.01(7)
O(1)−Mn−O(2)	88.69(7)	O(1)−Ni−O(2)	90.40(8)	O(1)−Zn−O(2)#1	89.99(7)
O(3)#1−Mn−O(2)#1	88.91(8)	O(3)#1−Ni−O(2)#1	90.25(9)	O(3)#1−Zn−O(2)	90.23(8)
O(3)−Mn−O(2)#1	91.09(8)	O(3)−Ni−O(2)#1	89.75(9)	O(3)−Zn−O(2)	89.77(8)
O(1)#1−Mn−O(2)#1	88.69(7)	O(1)#1−Ni−O(2)#1	90.40(8)	O(1)#1−Zn−O(2)	89.99(7)
O(1)−Mn−O(2)#1	91.31(7)	O(1)−Ni−O(2)#1	89.60(8)	O(1)−Zn−O(2)	90.01(7)
O(2)−Mn−O(2)#1	180.00(9)	O(2)−Ni−O(2)#1	180.00(10)	O(2)#1−Zn−O(2)	180.00(10)
O(14)−Cl(1)−O(12)	109.4(3)	O(14)−Cl(1)−O(13)	110.9(5)	O(14)−Cl(1)−O(12)	109.5(3)
O(14)−Cl(1)−O(13)	110.5(4)	O(14)−Cl(1)−O(12)	109.1(3)	O(14)−Cl(1)−O(13)	110.7(4)
O(12)−Cl(1)−O(13)	108.5(3)	O(13)−Cl(1)−O(12)	108.7(3)	O(12)−Cl(1)−O(13)	108.4(3)
O(14)−Cl(1)−O(11)	109.83(18)	O(14)−Cl(1)−O(11)	109.3(2)	O(14)−Cl(1)−O(11)	109.43(19)
O(12)−Cl(1)−O(11)	110.32(16)	O(13)−Cl(1)−O(11)	108.0(2)	O(12)−Cl(1)−O(11)	110.70(16)
O(13)−Cl(1)−O(11)	108.17(17)	O(12)−Cl(1)−O(11)	110.78(17)	O(13)−Cl(1)−O(11)	108.12(18)
C(8)−N(1)−C(2)	108.31(19)	C(8)−N(1)−C(2)	108.1(2)	C(8)−N(1)−C(2)	108.17(19)
C(8)−N(1)−C(9)	108.72(19)	C(8)−N(1)−C(9)	108.8(2)	C(8)−N(1)−C(9)	108.76(19)
C(2)−N(1)−C(9)	108.31(19)	C(2)−N(1)−C(9)	108.3(2)	C(2)−N(1)−C(9)	108.48(19)
N(1)−C(2)−N(3)	111.76(18)	N(1)−C(2)−N(3)	111.8(2)	N(1)−C(2)−N(3)	111.79(18)
C(4)−N(3)−C(10)	108.24(19)	C(10)−N(3)−C(4)	108.2(2)	C(10)−N(3)−C(2)	108.29(19)
C(4)−N(3)−C(2)	107.97(19)	C(10)−N(3)−C(2)	108.3(2)	C(10)−N(3)−C(4)	108.19(19)
C(10)−N(3)−C(2)	108.31(19)	C(4)−N(3)−C(2)	108.0(2)	C(2)−N(3)−C(4)	108.13(19)
N(3)−C(4)−N(5)	112.03(18)	N(3)−C(4)−N(5)	112.1(2)	N(3)−C(4)−N(5)	111.88(18)
C(6)−N(5)−C(4)	108.52(19)	C(6)−N(5)−C(4)	108.4(2)	C(6)−N(5)−C(9)	107.88(19)
C(6)−N(5)−C(9)	107.65(19)	C(6)−N(5)−C(9)	107.8(2)	C(6)−N(5)−C(4)	108.46(19)
C(4)−N(5)−C(9)	108.21(19)	C(4)−N(5)−C(9)	108.1(2)	C(9)−N(5)−C(4)	108.30(19)
N(5)−C(6)−N(7)	112.18(18)	N(5)−C(6)−N(7)	112.3(2)	N(5)−C(6)−N(7)	112.14(18)
C(10)−N(7)−C(6)	108.44(19)	C(6)−N(7)−C(10)	108.3(2)	C(6)−N(7)−C(10)	108.40(19)
C(10)−N(7)−C(8)	107.86(19)	C(6)−N(7)−C(8)	108.2(2)	C(6)−N(7)−C(8)	108.21(19)
C(6)−N(7)−C(8)	108.15(19)	C(10)−N(7)−C(8)	107.8(2)	C(10)−N(7)−C(8)	107.83(19)
N(1)−C(8)−N(7)	111.70(19)	N(1)−C(8)−N(7)	111.7(2)	N(1)−C(8)−N(7)	111.55(19)
N(1)−C(9)−N(5)	111.76(19)	N(1)−C(9)−N(5)	111.7(2)	N(5)−C(9)−N(1)	111.60(19)
N(7)−C(10)−N(3)	112.05(19)	N(3)−C(10)−N(7)	112.1(2)	N(3)−C(10)−N(7)	112.11(19)

[a] Symmetry transformations used to generate equivalent atoms #1: $-x, -y, -z$.

where α is the extent of conversion, E is the activation of energy at a particular α, R is the gas constant, and T_i is the absolute temperature. E is evaluated from the slope of the plot of $-\ln t_{\alpha,i}$ against $1/T_i$. Thus, E was evaluated at various extent of conversion, α. The dependencies of E on the extent of conversion are shown in Figure 8.

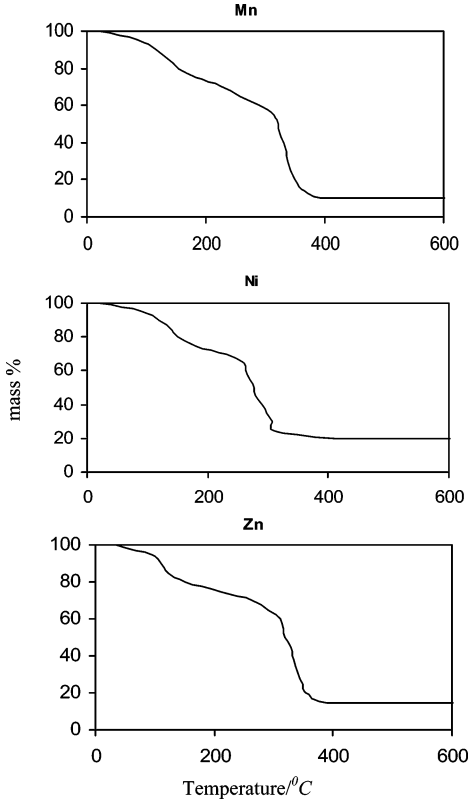

Figure 4. Nonisothermal TG of complexes in air at standard atmospheric conditions.

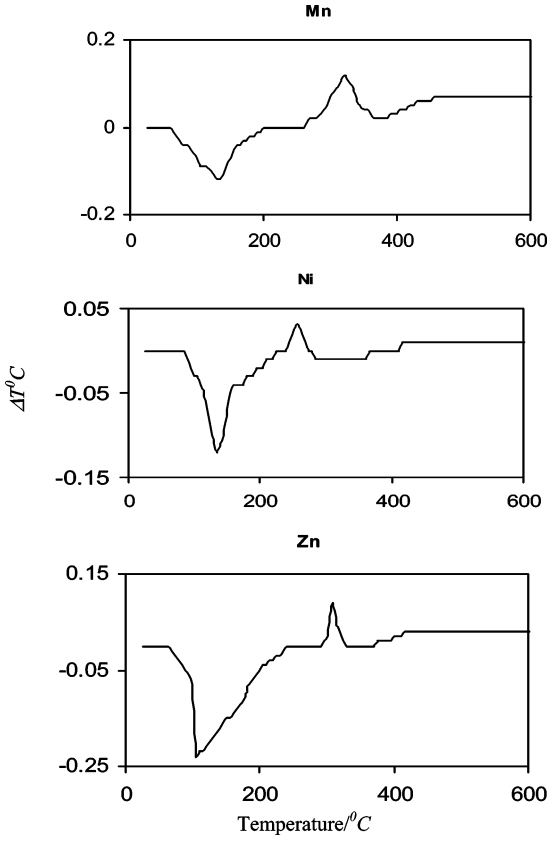

Figure 5. DTA thermogram of complexes in air at standard atmospheric conditions.

Results and Discussion

The crystal structures of the complexes are shown in Figures 1−3. The two HMTA molecules are attached with the metal ion through water molecules. The bonding between the HMTA and the water is clearly shown to be hydrogen bonding. Each HMTA is attached by hydrogen bonds between the nitrogen of HMTA and the hydrogen of the water molecule. The perchlorate ion is also attached to the water molecule via hydrogen bonding. Their crystal data, structure refinement, bond lengths, and bond angles, shown in Tables 1 and 2, clearly confirm the molecular formula of a single molecule $[M(H_2O-HMTA-H_2O)_2(H_2O-ClO_4)_2(H_2O)_2]$ (where M = Mn, Ni, and Zn).

The molar conductance (80−112 Ω^{-1} cm^2 mol^{-1}) of the complexes in water and DMSO at 10^{-2} to 10^{-4} molar concentrations proves their 1:2 electrolyte nature[28] and also support the structures given by X-ray crystallography.

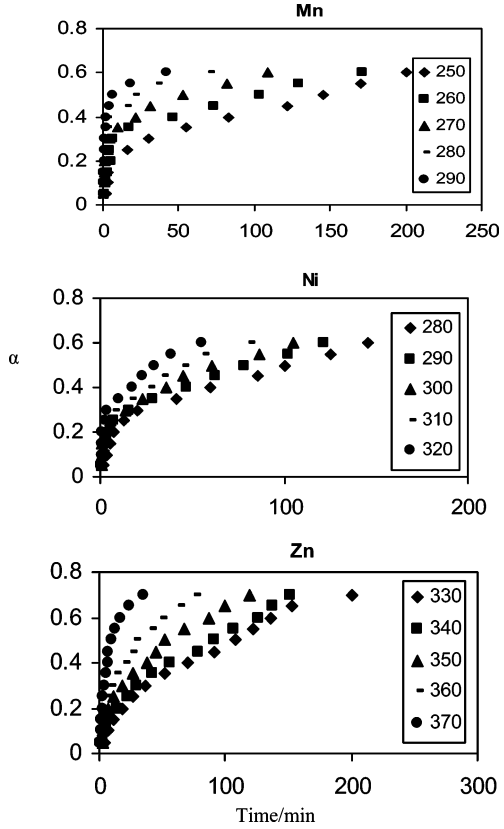

Figure 6. Isothermal TG of complexes.

TABLE 3: TG-DTA Phenomenological Data of the Complexes under Air Atmosphere

		TGA		DTA	
complex	step	*T* range/°C	decomposition (%)	peak temp./°C	nature
Mn complex	I	85−135	10.61	140	endo
	II	258−315	78.94	325	exo
Ni complex	I	90−135	10.55	135	endo
	II	259−280	78.20	260	exo
Zn complex	I	95−123	10.45	120	endo
	II	291−331	67.88	310	exo

TABLE 4: Explosion Delay (D_E/s), Activation Energy for Thermal Explosion (E^*/kJ mol^{-1}), and Correlation Coefficient (r) for the Complexes

	temp/°C						
complex	280 ± 1	300 ± 1	320 ± 1	340 ± 1	360 ± 1	E^*	r
Mn complex	85	68	61	50	40	26.5	0.9984
Ni complex	72	63	57	48	39	23.8	0.9953
Zn complex	107	90	85	60	45	27.8	0.9997

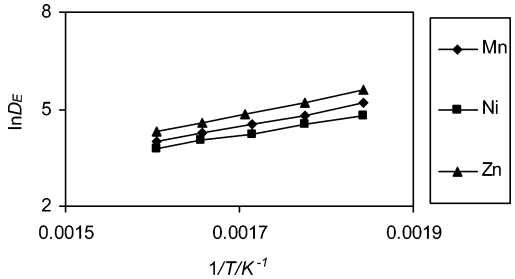

Figure 7. Plot of ln D_E vs $1/T$ for the complexes.

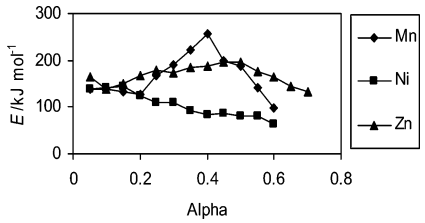

Figure 8. Dependence of activation energy (E) on the extent of conversion (α) for the complexes.

It is clear from TG and DTA data that all these complexes decompose in two steps (Table 3, Figure 4). The first step is the mass loss in the temperature range 85−139 °C, which corresponds to the loss of four water molecules, and the second step corresponds to the loss of two HMTA molecules and further interaction between the metal and perchlorate ion at higher temperatures to give finally the respective metal oxides with evolution of gaseous products. The rate of the thermolysis reaction is fast and highly exothermic in the second step, which is evident from by sharp DTA peaks presented in Table 3 and Figure 5. The endotherm in the first step of the decomposition is due to removal of four water molecules. Such findings have also been reported[5,6,7,11] during thermal decomposition of metal amine complexes. The decomposition pathways may be speculated as

$$[M(H_2O-HMTA-H_2O)_2(H_2O-ClO_4)_2(H_2O)_2] \xrightarrow{-4H_2O} [M(H_2O-HMTA)_2(H_2O-ClO_4)_2]$$

$$[M(H_2O-HMTA)_2(H_2O-ClO_4)_2] \rightarrow \text{metal oxide} + \text{gaseous products}$$

However, such a dissociation occurring in these complexes is difficult to detect by TG and DTA at atmospheric pressure. The reason for this is the the metal perchlorate is unstable at higher temperatures and would decompose with an instantaneously explosion. As shown in DTA, the expected endotherm corresponding to dissociation process may thus be completely overshadowed by exothermic process resulting in an overall exothermic effect.

In the analysis of kinetics from the isothermal TG data using the model fitting method, values of E obtained from different models for a particular sample are nearly equal but in the case of the Mn complex there is a larger deviation. It is difficult to assign a single value of E to a particular process taking place in such a complex solid-state decomposition. The isoconversional method shows that the thermolysis of these complexes is not as simple, as indicated by the model fitting method. As can be seen from Figure 8, the value of E changes with α but for all α, E for the Zn complex is generally higher than it is for Mn and Ni. The D_E data reported in Table 4 indicate that the time required for thermal explosion at a fixed temperature decreases in the order

$$[Zn(H_2O-HMTA-H_2O)_2(H_2O-ClO_4)_2(H_2O)_2] > [Mn(H_2O-HMTA-H_2O)_2(H_2O-ClO_4)_2(H_2O)_2] > [Ni(H_2O-HMTA-H_2O)_2(H_2O-ClO_4)_2(H_2O)_2]$$

All these complexes are stable at room temperature, but they explode when subjected to higher temperatures. The highest value of D_E and E^* for the Zn complex suggests that it is the most stable and the Ni complex is the least stable (Table 4 and Figure 7). The contributing factor for this trend may be due to a lower stability of the Ni (d^8 system) complex as compared to the Mn (half-filled d^5 system) complex.

Conclusions

The X-ray crystallography of the complexes shows that the HMTA is coordinated with a water molecule through the N atom of HMTA and the H atom of the water molecule. The perchlorate ion is also attached to metal through water. The thermal studies indicate that all these complexes undergo decomposition in two steps.

Acknowledgment. Thanks to the Head of the Chemistry Department of DDU Gorakhpur University for Lab facility use.

References and Notes

(1) Strohmeier, W.; Guttenberger, J. F. *Chem. Ber.* **1963**, *96*, 2112.
(2) Ahuja, I. S.; Tripathi, Shailendra. *Chem. Educ.* **1990**, Oct−Dec, 56.
(3) Ahuja, I. S.; Yadava, C. L.; Tripathi, S. *Indian. J. Chem.* **1989**, 167.
(4) Luttringhaus; A.; Kullick, W. *Tetrahedron Lett.* **1959**, *10*, 13.
(5) Singh, G.; Singh, C. P.; Mannan, S. M. *J. Hazarad. Mater.* **2005**, *122*, 111.
(6) Singh, G.; Singh, C. P.; Mannan, S. M. *Thermochim. Acta* **2005**, *21*, 437.
(7) Singh, G.; Pandey, D. K. *Combust. Flame* **2003**, *135*, 135.
(8) Singh, G.; Pandey, D. K. *J. Therm. Anal. Cal.* **2005**, *82*, 353.
(9) Singh, G.; Pandey, D. K. *Propellants Explos. Pyro.* **2003**, *28*, 5.
(10) Singh, G.; Prem Felix, S.; Pandey, D. K. *Thermochim. Acta* **2004**, *411*, 61.
(11) Singh, G.; Singh, C. P.; Mannan, S. M. *J. Hazarad. Mater.* **2006**, *A135*, 10.
(12) Singh, G; Baranwal, B. P.; Kapoor, I. P. S.; Kumar, D.; Singh, C. P.; Frohlich, Roland, J. *Therm. Anal. Cal.*, in press.
(13) Patil, K. C.; Pai, V. R.; Verneker, V. M. S. *Combust. Flame* **1975**, *25*, 387.
(14) Sawant, S. Y.; Kannan, K. R.; Verneker, V. M. S. In *Thirteenth National Symposium on Thermal Analysis BARC*, Mumbai, India, 2002.
(15) Singh, G.; Kapoor, I. P. S.; Pandey, D. K. *J. Energ. Mater.* **2002**, *20*, 223.
(16) Singh, G.; Pandey, D. K. *Propellants Explo. Pyro.* **2003**, *28*, 5.
(17) Otwinowski, Z.; Minor, W. *Methods Enzymol.* **1997**, *276*, 307.
(18) Sheldrick, G. M. *Acta Crystallogr. A* **1990**, *46*, 467.
(19) Sheldrick, G. M. SHELXL-97, Program for Crystal Structure Refinement, University of Gottingen, Germany, 1997.
(20) Keller, E. SCHAKAL − A Computer program for the Graphic Representation of Molecular and Crystallographic Models, University of Freiburg, Germany, 1997.
(21) Singh, G.; Singh, R. R. *Res. Ind.* **1978**, *23*, 92.
(22) Singh, G.; Kapoor, I. P. S.; Vasudeva, S. K. *Indian J. Technol.* **1991**, *29*, 589.
(23) Semenov, N. *Chemical Kinetics and Chain Reactions*; Clarendon Press: Oxford, U.K., 1935; Chapter 18.
(24) Freeman, E. S.; Gordon, S. *J. Phys. Chem.* **1956**, *60*, 867.
(25) Zinn, J.; Rogers, R. N. *J. Phys. Chem.* **1962**, *66*, 2646.
(26) Singh, G.; Felix, Prem, S.; Pandey, D. K. *Thermochim. Acta* **2004**, *411*, 61.
(27) Vyazovkin, S.; Wight, C. A. *J. Phy. Chem. A* **1997**, *101*, 8279.
(28) Geary, W. J. *Coord. Chem. Rev.* **1971**, *7*, 81.